Sub-barrier Fusion Cross Sections with Energy Density Formalism

Muhammad Zamrun F., K. Hagino, N. Takigawa

Department of Physics, Tohoku University, 980-8578 Japan

Abstract. We discuss the applicability of the energy density formalism (EDF) for heavy-ion fusion reactions at sub-barrier energies. For this purpose, we calculate the fusion excitation function and the fusion barrier distribution for the reactions of ^{16}O with ^{154,144}Sm,^{186}W and ^{208}Pb with the coupled-channels method. We also discuss the effect of saturation property on the fusion cross section for the reaction between two ^{64}Ni nuclei, in connection to the so called steep fall-off phenomenon of fusion cross sections at deep sub-barrier energies.

Keywords: heavy-ion fusion, fusion cross section, energy density formalism, coupled-channels method, Skyrme functional
PACS: 21.60.Jz,24.10.Eq,25.60.Pj

INTRODUCTION

The internuclear potential is one of the most important ingredients in describing heavy-ion reactions. The double folding model (DFM) [1,2] has been widely used in order to construct it microscopically. This model uses the sudden approximation i.e., the assumption that the density of each colliding ion is kept at all distances during the collision. The effect of nucleon exchange between the colliding nuclei is partly taken into account in this model through the so called knock-on exchange potential. Since it does not fully include the exchange effect, the saturation property of nuclear matter is respected only partly.

Since heavy-ion fusion reactions probe the region inside the Coulomb barrier, where the projectile and target nuclei appreciably overlap with each other, the effect of saturation plays an important role [3]. There is actually a model for internuclear potential which consistently takes account of the saturation property of nuclear matter. That is the energy density formalism (EDF) [4-10], firstly proposed by Brueckner et al. [4]. This model constructs the internuclear potential from an energy functional for a dinucleus system. Earlier studies have shown that this method can account for the elastic scattering of ^{16}O+^{16}O reaction [4] and the experimental barrier height for many systems [5]. Brink and Stancu have investigated intensively the applicability of this method using the Skyrme energy functional [6-8]. They also showed that the EDF potential is consistent with the proximity potential. A similar conclusion was also obtained in Ref. [9] using a higher-order Thomas-Fermi approximation for the kinetic energy and spin orbit densities. More recently, the EDF was applied to the simplified coupled-channels calculations for heavy-ion fusion reaction at sub-barrier energies [10].

In this contribution, we apply the EDF to heavy-ion fusion reactions and perform the full order coupled-channels calculations. In particular, we analyze the fusion reactions

of ^{16}O with ^{154,144}Sm,^{186}W and ^{208}Pb. We also discuss the effect of saturation property on the fusion cross section at energies close to, and well below, the Coulomb barrier for ^{64}Ni+^{64}Ni fusion reaction, for which the so called steep fall-off phenomenon was recently reported [11].

ENERGY DENSITY FORMALISM

In the energy density formalism, the internuclear potential is assumed to be given by an energy density for the dinuclear system consisting of the target and projectile nuclei. If one takes the frozen density approximation, it is given as

$$V(R) = \int \{\varepsilon[\rho_p^{(P)}(\vec{r}) + \rho_p^{(T)}(\vec{r},\vec{R}), \rho_n^{(P)}(\vec{r}) + \rho_n^{(T)}(\vec{r},\vec{R})] - \varepsilon[\rho_p^{(P)}(\vec{r}), \rho_n^{(P)}(\vec{r})] - \varepsilon[\rho_p^{(T)}(\vec{r},\vec{R}), \rho_n^{(T)}(\vec{r},\vec{R})]\}\, d\vec{r}. \quad (1)$$

Here $\varepsilon[\rho_p(\vec{r}), \rho_n(\vec{r})]$ is the energy density functional, and $\rho_p^{(P,T)}(\vec{r})$ and $\rho_n^{(P,T)}(\vec{r})$ are the proton (p) and neutron (n) density distributions of the projectile (P) and target (T) nuclei, respectively. $\rho(\vec{r},\vec{R})$ represents the density whose center is at $\vec{R}$. The first term in eq.(1) represents the total energy of the system when two ions are separated by distance R, while the second and the third terms are the ground state energy of each ion. In this contribution, we use the Skyrme functional for $\varepsilon[\rho_p(\vec{r}), \rho_n(\vec{r})]$. See Refs. [6,12,13] for its explicit form.

We estimate the kinetic energy and spin orbit densities in the semi-classical extended Thomas-Fermi approximation [9,14]. In this way, the internuclear potential is entirely determined by the density distributions for the colliding nuclei. We evaluate them with the Skyrme-Hartree-Fock (SHF) method using the same parameter set of the Skyrme interaction as that we employ for calculating the internuclear potential. The pairing correlation is taken into account in the BCS approximation with the constant gap approach. We take $\Delta_p = \Delta_n = 11.2/\sqrt{A}$ for this purpose. We fit the SHF density with a modified Fermi function in evaluating the internuclear potential according to Eq.(1). We introduce an overall scaling factor to the potential obtained in this way so as to reproduce the experimental data.

RESULTS AND DISCUSSIONS

Coupled-channels calculations with EDF

We now apply the EDF to the reactions of ^{16}O with ^{154,144}Sm,^{186}W and ^{208}Pb. In the following calculations, we use the SkM* parameter set [15]. This parameter set gives the incompressibility of nuclear matter which is close to the experimental value [14] and has been successfully used for the description of ground state properties for many nuclei.

The channel coupling does not play so important role at energies above the Coulomb barrier. We therefore first perform the single-channel calculation for each system by ignoring nuclear intrinsic excitations and determine an overall normalization factor of

the EDF potential in order to reproduce the experimental fusion cross sections at high energies. In order to facilitate the coupled-channels calculations, which are essential at energies below the Coulomb barrier, we simulate the surface region of the resultant potential by Woods-Saxon form. The normalization factor (N), the optimum Woods-Saxon parameters (V_0, r_0, a), and the corresponding Coulomb barrier height (V_B) for each system are summarized in Table 1. We notice from Table 1 that the EDF potential provides the surface diffuseness parameter a of around 0.7 fm, which is similar to the result of double folding model [2] and is almost independent of the system.

In performing the coupled channels calculations, we introduce the excitation operator for the intrinsic excitation, through the radius parameter of the target nucleus in the standard way. We used the computer code CCFULL [16] for numerical calculations.

TABLE 1. Normalization factor and optimum Woods-Saxon parameters for the EDF potential for the ^{16}O+^{144,154}Sm, ^{186}W, and ^{208}Pb reactions.

System	N	V_0 **(MeV)**	r_0 **(fm)**	a **(fm)**	V_B **(MeV)**
^{16}O+^{144}Sm	1.07	66.57	1.140	0.74	61.73
^{16}O+^{154}Sm	1.31	82.66	1.144	0.75	59.54
^{16}O+^{186}W	1.37	86.86	1.152	0.73	69.02
^{16}O+^{208}Pb	1.47	95.20	1.150	0.74	74.73

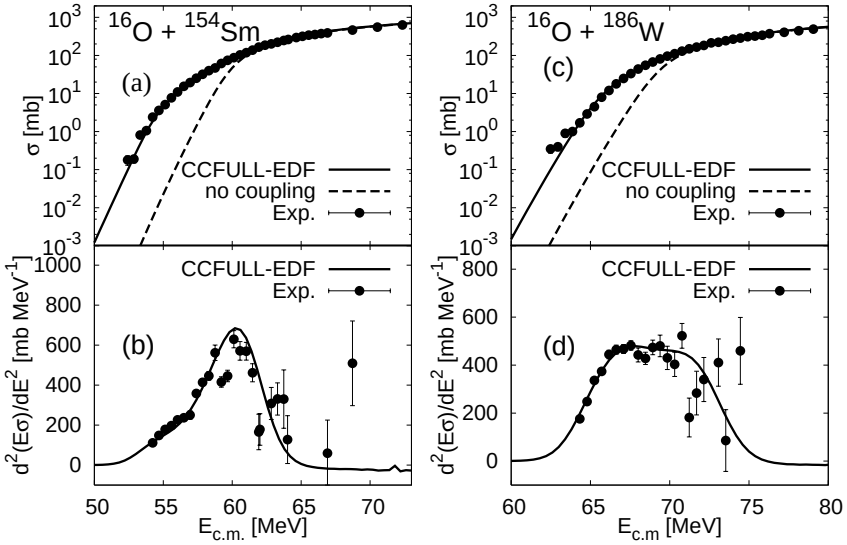

FIGURE 1. Fusion cross sections and fusion barrier distributions for the ^{16}O+^{154}Sm (1(a) and 1(b)) and ^{16}O+^{186}W (1(c) and 1(d)) reactions. Experimental data are taken from Ref. [18].

Figures 1(a) and 1(c) show the fusion cross sections for ^{16}O+^{154}Sm and ^{186}W reactions, respectively, as functions of the incident energy in the center of mass frame. The corresponding fusion barrier distributions are shown in Figs. 1(b) and 1(d). We include the deformation parameters up-to β_6 of the target nucleus in both cases [17]. The ground state rotational band up-to the 10^+ and 14^+ member of the ^{154}Sm and ^{186}W, respectively, is taken into account. We determine the deformation parameters by fitting to the experimental fusion cross sections. The resultant deformation parameters are $\beta_2 = 0.33$,

$\beta_4 = 0.035$ and $\beta_6 = 0.033$ for ^{154}Sm, and $\beta_2 = 0.335$, $\beta_4 = -0.045$, and $\beta_6 = 0.018$ for ^{186}W. These values are similar to those obtained in [17]. The figure clearly shows that our calculations well reproduce the experimental data.

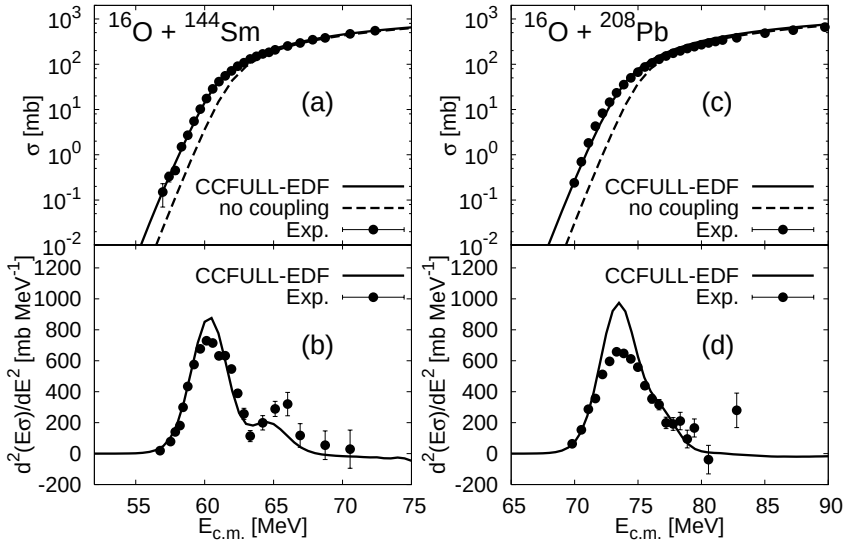

FIGURE 2. Same as Fig. 1, but for ^{16}O+^{144}Sm (2(a) and 2(b)) and ^{16}O+^{208}Pb (2(c) and 2(d)) reactions. The experimental data are taken from Refs. [18,19].

We next study the fusion reactions with spherical target nuclei, that is ^{16}O+^{144}Sm and ^{208}Pb reactions. We include the couplings to the 2^+ and 3^- vibrational states in ^{144}Sm and to the 3^- and 5^- states in ^{208}Pb. We estimate the deformation parameters from the experimental B(E2), B(E3) and B(E5) values. The excitation energies and deformation parameters are $E_2 = 1.66$ MeV, $\beta_2 = 0.11$ and $E_3 = 1.81$ MeV, $\beta_3 = 0.205$ for ^{144}Sm and $E_3 = 2.615$ MeV, $\beta_3 = 0.161$ and $E_5 = 3.928$ MeV, $\beta_5 = 0.056$ for ^{208}Pb. The results of the coupled channels calculations are compared with the experimental data in Fig. 2. We see again that the present calculations well reproduce the experimental data of the fusion cross sections for both systems.

Effect of incompressibility

We next discuss the effect of incompressibility of nuclear matter on the fusion cross section. We are especially interested in the connection between the nuclear incompressibility and the steep fall-off problem at deep sub-barrier energies. We therefore choose the fusion reactions of two ^{64}Ni nuclei, whose fusion excitation function shows the steep fall-off problem [11]. Figures 3(a) and 3(b) show the total potential and the nuclear potential for this system obtained with EDF using three different Skyrme parameters. The solid, dashed, and dotted lines have been obtained with SIII (K_∞=355.4 MeV) [20], SGI (K_∞=269 MeV) [21], and SkM* (K_∞=216.7 MeV) [15] parameter sets, respectively. One observes in Fig. 3(b) that the nuclear potential tends to be shallower and more repulsive with increasing incompressibility. The fusion excitation function slightly reflects these differences as shown in Figs. 3(c) and 3(d).

A more important observation in connection with the steep fall-off problem is that the nuclear potential, hence also the total potential, have a much shallower depth at the potential minimum compared to the corresponding potentials given by the double folding model (DFM) irrespective to the choice of the force parameters. The DFM using the M3Y force and the same densities as those in the present EDF does not actually show a potential pocket, and the depth is as large as -2500 MeV and -2250 MeV for the nuclear and total potentials, respectively. The EDF using the Skyrme force yields a shallow potential irrespective to the parameter sets, because the nuclear saturation property is taken into account to some extent for all of them. Interestingly, as shown in Fig.3(a), the minimum energy of the potential pocket nearly equals to that discussed by Misicu and Esbensen [3], who modified the DFM by adding a repulsive term in order to explain the steep-fall off phenomenon. The minimum position, which is about 80 MeV in the present calculation, is comparable to energy $E_S \sim 87$ MeV, where the data of the fusion excitation function start to fall steeply.

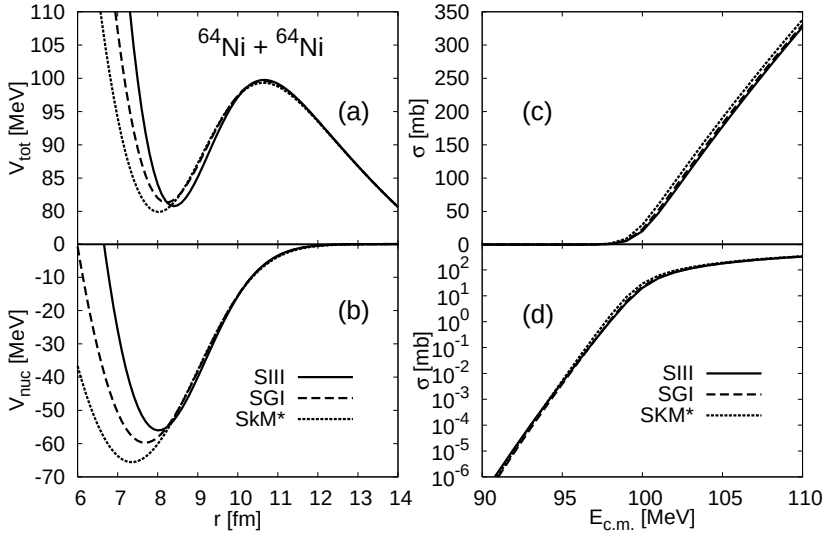

FIGURE 3. The total (Fig. (3a)) and nuclear (Fig. (3b)) potentials for ^{64}Ni+ ^{64}Ni reaction calculated with three different Skyrme forces. Figs. 3(c) and 3(d) show the fusion cross sections obtained with these potentials.

CONCLUSIONS AND FURTHER PERSPECTIVES

We have performed the coupled-channels calculations based on the EDF for ^{16}O + ^{154,144}Sm,^{186}W and ^{208}Pb reactions. We have shown that our calculations reproduce well the experimental data of the fusion excitation function as well as the fusion barrier distribution for these systems. Also, using ^{64}Ni+^{64}Ni reactions, we have shown that the EDF potential given by the Skyrme energy density has a much shallower depth than the standard DFM and suggested that the nuclear saturation property may provide an origin of the steep fall-off phenomenon at deep sub-barrier energies.

In the present studies, we employed the frozen density approximation, where the total density of the system is simply given by the sum of the densities of the projectile

and target nuclei. This approximation leads to the unphysically high density matter when two colliding nuclei completely overlap and may break down inside the Coulomb barrier. This problem can be, at least partly, resolved by respecting the Pauli principle, i.e. the role of antisymetrization in the calculation of the densities of two colliding nuclei [6,22]. Another problem which should be examined is the adiabaticity of the fusion reactions. The frozen density approximation implies that the reaction takes place suddenly. However, it is not obvious whether the sudden approach holds to a good approximation for the reactions at low energies. The opposite limit is the adiabatic approximation, where the densities of the colliding ions change dynamically at every instant. The EDF can accommodate both limits in a natural way, and is suited to examine the adiabaticity of the reactions. In connection with the steep fall-off problem, it is an interesting question to see at what energy the present sudden approximation breaks down and whether the potential minimum still remains shallow even if one goes beyond the sudden approximation. A work towards these directions is now in progress.

ACKNOWLEDGMENTS

This work was partly supported by The 21st Century Center of Excellence Program "Exploring New Science by Bridging Particle-Matter Hierarchy" of the Tohoku University, and Monbukagakusho Scholarship from the Japanese Ministry of Education, Culture, Sports, Science and Technology. This work was also supported by the Grant-in-Aid for Scientific Research, Contract No. 16740139 from the Japanese Ministry of Education, Culture, Sports, Science, and Technology.

REFERENCES

1. G.R. Satchler and W.G. Love, *Phys. Rep.* **55**, 183 (1979).
2. I.I. Gontchar, D.J. Hinde, M.Dasgupta, and J.O. Newton, *Phys. Rev. C***69**, 024610 (2004).
3. S. Misicu and H. Esbensen, *Phys. Rev. Lett.* **96**, 112701 (2006).
4. K.A. Brueckner, J.R. Buchler and M.M. Kelly, *Phys. Rev.* **173**, 944 (1968).
5. C. Ngo et al., *Nucl. Phys. A***240**, 353 (1975).
6. D.M. Brink and Fl. Stancu, *Nucl. Phys. A***243**, 175 (1975).
7. Fl. Stancu and D.M. Brink, *Nucl. Phys. A***270**, 236 (1976).
8. D.M. Brink and Fl. Stancu *Nucl. Phys. A***299**, 321 (1978).
9. A. Dobrowolski, K. Pomorski and J. Bartel, *Nucl. Phys. A***729**, 713 (2003).
10. Min Liu, et al., *Nucl. Phys A***768**, 80 (2006).
11. C.L. Jiang, et al., *Phys. Rev. Lett.* **93**, 012701 (2004); *Prog. Theor. Phys. Suppl.* **154**, 61 (2004).
12. D. Vautherin and D.M. Brink, *Phys. Rev. C***5**, 626 (1972).
13. J. Bartel and K. Bencheikh, *Eur. Phys. J. A***14**, 179 (2002).
14. M. Brack, C. Guet and H.B. Hakanson, *Phys. Rep.* **123**, 275 (1985).
15. J. Bartel, P. Quentin, M. Brack, C. Guet and H.B. Hakanson, *Nucl. Phys. A***386**, 79 (1982).
16. K. Hagino, N. Rowley and A.T. Kruppa, *Comput. Phys. Commun.* **123**, 143 (1999).
17. Tamanna Rumin, K. Hagino and N. Takigawa, *Phys. Rev. C***61**, 014605 (1999).
18. J.R. Leigh et al., *Phys. Rev. C***52**, 3151 (1995).
19. C.R. Morton et al., *Phys. Rev. C***60**, 044608 (1999).
20. M. Beiner, H. Flocard, Nguyen Van Giai and P. Quentin, *Nucl. Phys. A***238**, 29 (1975).
21. Nguyen Van Giai and H. Sagawa, *Phys. Lett. B***106**, 379 (1981).
22. K. Hagino and K. Washiyama, contribution to this conference, e-print: nucl-th/0605017.